Online ISSN: 2383-0042

Iranian Journal of Materials Forming

Journal Homepage: http://ijmf.shirazu.ac.ir

Research Article

Forming of Archimedean Spiral Bipolar Plates using Hot Gas Forming Process and its Characteristics Evaluation

S. J. Hashemi [1], A. H. Roohi[2*] and R. Kermanshahi[3]

[1] Department of Mechanical Engineering, Faculty of Enghelab-e Eslami, Tehran Branch, Technical and Vocational University (TVU), Tehran, Iran
[2] Department of Mechanical Engineering, Faculty of Industrial and Mechanical Engineering, Qazvin Branch, Islamic Azad University, Qazvin, Iran
[3] Department of Mechanical Engineering, Kar Higher Education Institute, Qazvin, Iran

ARTICLE INFO

Article history:

Received 10 March 2020
Reviewed 27 September 2020
Revised 4 October 2020
Accepted 18 October 2020

Keywords:

Bipolar plates
Hot gas forming process
Channel depth
Thinning percentage
Parametric study

ABSTRACT

Membrane fuel cells are considered as highly efficient energy generators that do not cause environmental pollutions. In this regard, bipolar plates are the main component of the fuel cells given that they have the following required characteristics; good flexural strength and high electrical conductivity. In the current study, some experiments have been carried out to investigate the forming process of Archimedean spiral aluminum bipolar plates. Thus, an experimental setup is designed and fabricated in order to make the process possible. Additionally, the effects of process parameters on the geometrical characteristics of the product are studied using a response surface methodology and as a result, the optimum values are specified. Thus, 5 different levels were considered for 3 input parameters. Experimental results show that gas temperature has the most significant influence on the channel depth and thinning percentage, whereas the time of applying gas pressure has the least effect. In fact, when the gas temperature increases from 200˚C to 400˚C, the channel depth increases from 0.28 to 0.84 mm. Finally, the optimum process parameters are specified as follows: gas pressure of 38 bar, temperature of 308˚C, and process time of 10 sec.

1. Introduction

Fuel cells are devices utilized to convert chemical energy into direct electrical current. An electrochemical reaction between oxygen and hydrogen is performed through the fuel cells and a by-product of water is also derived. No pollutant yields, as a result of this reaction inside the fuel cell. The fuel cell stack is a multi-layered structure that consists of unit cells and two endplates. The fuel cell unit cell includes membrane electrode assemblies, gas diffusion layers and bipolar plates [1]. The bipolar plates are the main component of a fuel cell that cost about 30-35% and weigh 60-80% of a stack [2].

The main tasks of each bipolar plates are as follows: transmission of electricity from one cell to another, conduction of heat and water produced in the cell, and providing channels for reaction gases including oxygen and hydrogen [3]. Once such tasks are completed, the bipolar plates should have high mechanical strength, high chemical stability, appropriate electrical conductivity, low weight, low thickness and gas permeability [4]. The US office of energy efficiency and renewable energy has identified the technical properties needed to meet the requirements. These properties are shown in Table 1 [5].

* Corresponding author
E-mail address: Amir.roohi@qiau.ac.ir (A. H. Roohi)
https://doi.org/10.22099/ijmf.2020.36696.1154

Table 1. US-DOE target values for bipolar plates

Functional requirement	Target values
Flexural strength	> 25 MPa
Electrical conductivity	> 100 $S.cm^{-1}$
Areal specific resistance	< 30 $m\Omega.cm^2$ @ 1.4 MPa
Gas permeability	< 2×10^{-6} $cm^3.(s.cm^2)^{-1}$
Corrosion resistance	< 1 $\mu A.cm^2$

Due to the large number of bipolar plates used in stacks, cheap methods and materials are required to produce these plates. One of the best materials to fabricate the bipolar plates is graphite, which has good electrical properties and high chemical stability. However, graphite plates are fragile and have low machining capabilities [6]. On the other hand, metallic bipolar plates are an appropriate replacement for graphite plates, given their suitable mechanical properties and high electrical and thermal conductivity [3, 7]. In recent years, different methods have been used to form the metal sheets in the form of parallel channels in the bipolar plates. Nikam et al. [8] used roll forming grooved rollers to form copper sheets while Jin et al. [9] used a dynamic force with a square wave, which is applied on the stamping die, to form a bipolar sheet indicating that as the number of loading cycles increases, the depth of the channel increases. Hu et al. [10] investigated the effect of geometrical parameters of the die, as well as, process parameters on the material flow into the bipolar plates in the stamping process, using finite element simulation. The results showed that low and high punch speed causes shrinkage and crack propagation, respectively. Brady et al. [11] used a stamping process to produce bipolar sheets from stainless steel foils and then performed laser welding operations on it.

Some researches have been also carried out on the rubber pad forming process of bipolar sheets. In this process, a flexible rubber pad is used to form a sheet metal, where no precise assembly of the process component is required. This process could increase the formability of the sheet, due to the flexible contact between the sheet and the rubber pad [12, 13]. Peng et al. [14] conducted an experimental and numerical study of the rubber pad forming of bipolar sheets in micro/meso scales. Based on the results of this study, in which a rubber punch was used, small grain sizes are required to achieve maximum formability. Dirikolu et al. [15] numerically and experimentally investigated the effects of process parameters, including rubber hardness, sheet material type and friction coefficient, as well as geometrical parameters of the die on the channel depth. Liu et al. [16] compared the rubber pad forming of bipolar plates in the concave and convex forms using numerical and experimental methods. Kolahdooz et al. [17] used a numerical simulation and design of experiment methodology to determine the effective parameters in the bipolar plate production using a rubber pad forming process. According to their results, the draft angle, the outer corner radius of the channel and the coefficient of friction are the most effective parameters in the process. On the other hand, the forming of bipolar plates using the hydroforming process has also been studied. Koc et al. [18] developed a new method for fabrication of bipolar plates based on the fluid pressurized approach. Peng et al. [19] numerically investigated the simultaneous construction of two sheets using fluid pressure in order to obtain optimal geometrical parameters of the channels to achieve the most formability. Dundar et al. [20] compared the corrosion resistance of bipolar plates shaped by the stamping and hydroforming process. Their results showed that sheets were formed with less fluid pressure were more resistant to corrosion. Hung et al. [21] investigated the construction of bipolar plates with a high aspect ratio (i.e. depth to width ratio) using a high pressure hydroforming process. They reached the ratio of 0.48 for sheets with the thickness of 0.1. Palumbo et al. [22] also performed the hydroforming process of bipolar plates of AA6061 aluminum at elevated temperatures.

The aluminum alloys have been used in the automotive and aerospace industries, due to the necessity of producing low weight parts with high corrosion resistance. The main difficulty about the application of these alloys is their low formability at ambient temperatures [23]. As a matter of fact, because of the presence of alloying elements in aluminum alloys, these plates have lower formability at low temperatures. One of the ways to enhance their formability is to raise the temperature during the process. Thus, the hot gas forming process could be used to form the aluminum alloys and high strength steels, as well [24]. In this process, the metal sheet is first warmed up to a high temperature and then, deformed by applying a neutral gas pressure. In fact, the gas pressure is replaced with the punch in the stamping process. As a result of enhanced formability at elevated temperatures, the forming of bipolar plate channels with a higher depth is feasible. In addition, there is no need for higher values of the pressure to form the sheet as the flow stress of the material is reduced. Keigler et al. [25] studied the formability, wall thickness distribution and microstructure of the samples after conducting the hot gas forming process by numerical simulation with LS-DYNA software. The optimal process parameters were obtained using their results. Zhu-bin et al. [26, 27] studied the microstructure and formability of the AA6061 aluminum alloy and the way of the bursting, which it experiences at high temperatures. In this study, the free bulging of the aluminum tubes were performed using the hot gas forming method at temperature ranges from 350°C to 500°C. Liu gang et al. [28] investigated the warm thin-walled tube hydroforming within non-uniform temperature field with large expansion ratio. Finally, Maeno et al. [29] increased the temperature of aluminum tubes to 500°C and examined the bulging of the tube using the hot gas pressure. It's worth mentioning that using DOE methods in statistical investigation of forming and manufacturing methods are considered in common. In this regard, some studies are as follows: Vahdati et al. [30] have used RSM methodology and desirably function method in order to optimize the mechanical strength of the Al7075 alloys in solid-state welding processes. Roohi et al. [31] used a full factorial design of experiment in order to find the optimized hot metal gas forming process parameters on the sandwich panel products. In another study, Vahdati et al. [32] studied the yield strength and hardness of surface composites in thermo-mechanical processes. Mostafapour et al. [33] used a multi-response optimization method to investigate the mechanical and metallurgical properties of the deposition of Al7075-T6 coating on Al2024-T351 substrates.

So far, there are limited investigations about the hot gas forming process of bipolar plates. In this manuscript, the hot gas forming of aluminum sheets needed in order to produce bipolar plates with the Archimedean pattern has been experimentally investigated. Thus, a set of experimental setup is designed to produce the bipolar plate products. The effect of the process parameters, including temperature, time and maximum gas pressure, on the channel depth has been studied. Results show that gas temperature has the most significant influence on the channel depth and thinning percentage, whereas the time of applying gas pressure has the least effect. The thickness distribution of the products has been inspected and finally, the optimal values of the parameters have been determined.

2. Experimental Procedure

The sheets used in this paper were of aluminum alloy AA1050 with a thickness of 300 microns. The forming die of the Archimedean-pattern bipolar plates is shown in Fig. 1. This setup includes an upper die and a lower die. The channel pattern is placed on the lower die and the two halves are fastened by four screws. The width and depth of each channel is as well as the distance between the channels are all measured at 1.5 mm. The channel corner radius is 0.2 mm and the walls are completely vertical (see Fig. 1). As it is obvious, the channel pattern is in Archimedean spiral-shaped. When utilizing the bipolar plate in the fuel cell, gas enters from one side and leaves from the other side. Three heating elements of sparkling type in the lower die have been used to heighten the die's temperature to the desired level. The components of the hot gas forming unit are shown in Fig. 2. First, the aluminum sheet is placed on the lower die, and then the upper die is placed on it and tightened with screws. The movement of the edges of the sheet is restricted by the positioning between the two dies. The die temperature is increased by connecting the electrical current to the heating elements and measured by a thermocouple, which is in contact with the sheet. The pressure required to form the sheet is supplied by a compressed air cylinder with the maximum pressure of 150 bar that is connected by a hose to the gas inlet manifold in the upper die. A regulator with a precision of 1 bar has been used to adjust the output pressure of the cylinder. The rise in pressure during the process is done in such a way that an almost linear graph in time is satisfied. It is worth mentioning that the process parameters and their corresponding level during the experimentations are listed in Table 2.

Table 2. Process parameters and their level during the experimentations

Parameter	1st Level	2nd Level	Central Level	4th Level	5th Level
Temperature [˚C]	200	250	300	350	400
Pressure [bar]	20	25	30	35	40
Process time [s]	10	15	20	25	30

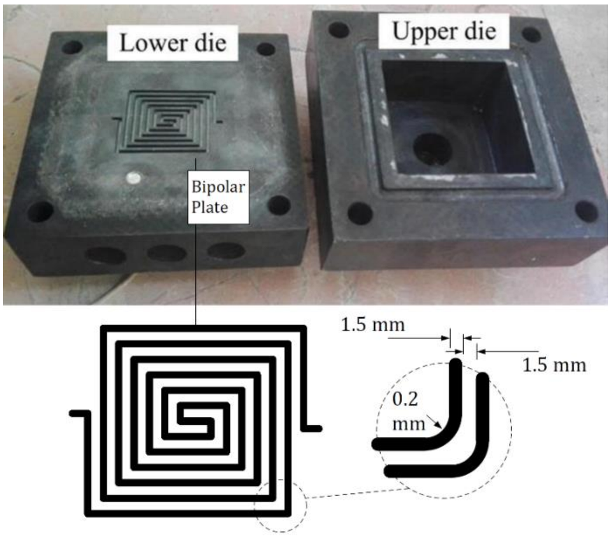

Fig. 1. Hot gas forming dies to produce bipolar plates.

3. Results and Discussion

The effects of input process parameters, including temperature, time and final applied gas pressure is investigated on the output parameters, that are the channel depth and the thinning percentage. With regard to the consideration of 5 levels for each of the parameters (in accordance with the response surface methodology-central composite design of the experiment), 20 experiments were carried out. Due to the fact that the depth of the channels in each sample is not the same, the depth of the channel in the middle point was measured for all specimens. The cross-section of the central channel for a random sample is illustrated in Fig. 3. This figure also shows how the depth of the channels is measured. As shown in Fig. 3, the maximum thinning is observed in the corner of the channel. As a result, the thickness of all samples was measured at this point. Table 3 lists the parameter values in each experiment and the corresponding channel depth and the thinning percentage. The specimens were formed at 300°C and other different process parameters are shown in Fig. 4.

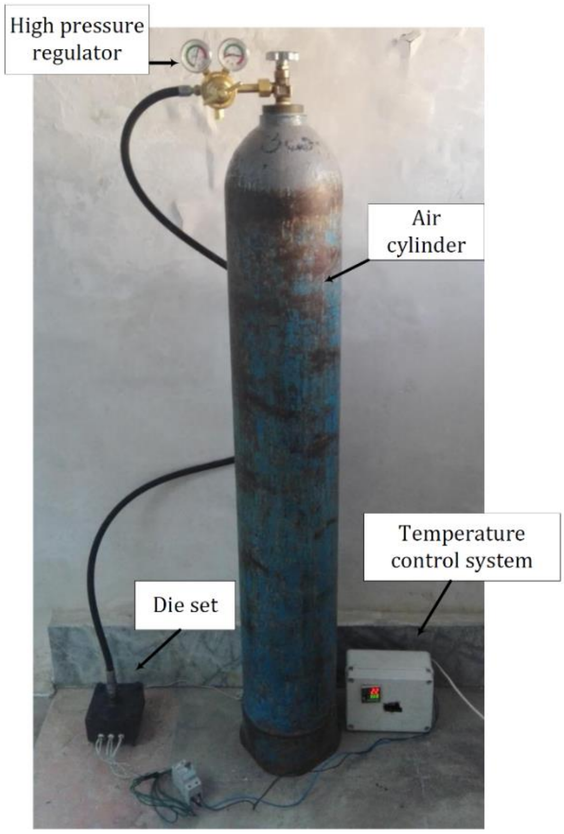

Fig. 2. The experimental setup components of hot gas forming process.

Table 3. Experimental results of the hot gas forming process

No. of Experiment	Temperature [˚C]	Pressure [bar]	Process time [s]	Thinning (%)	Channel depth (mm)
#1	200	30	20	7.6	0.32
#2	350	25	15	22.3	0.53
#3	300	30	20	17.9	0.45
#4	300	30	20	19	0.47
#5	300	30	20	18.5	0.44
#6	300	30	10	15.8	0.35
#7	300	20	20	15.6	0.34
#8	350	35	25	27.2	0.74
#9	250	25	25	10.6	0.31
#10	300	40	20	21.5	0.51
#11	400	30	20	29.5	0.79
#12	250	25	15	10.3	0.31
#13	350	25	25	23.1	0.56
#14	300	30	30	18.7	0.45
#15	300	30	20	17.9	0.43
#16	250	35	15	11.3	0.31
#17	250	35	25	13.3	0.33
#18	300	30	20	17.5	0.44
#19	300	30	20	18.2	0.45
#20	350	35	15	25.3	0.72

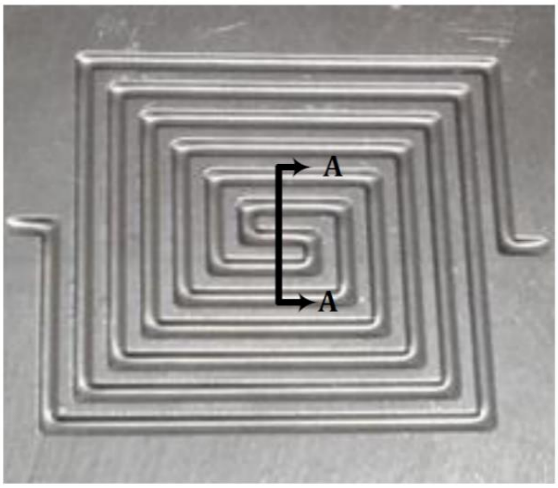

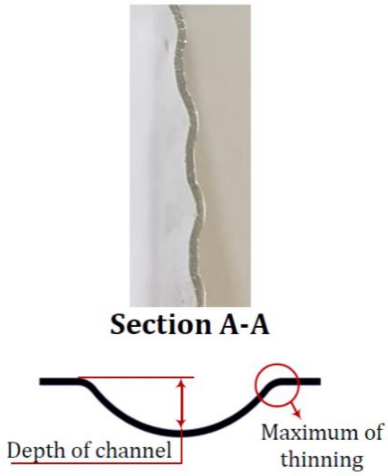

Fig. 3. Cross-section of the central channel (Experiment number: #10).

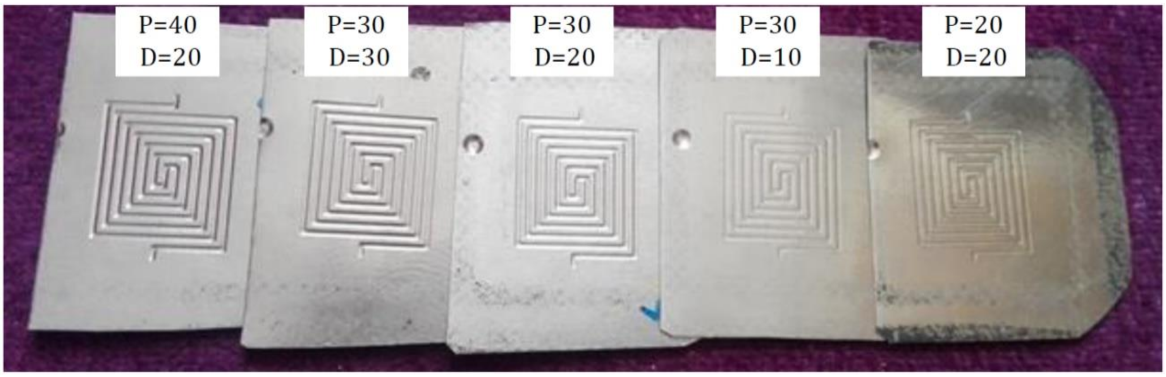

Fig. 4. Formed bipolar plates at the temperature of 300˚C.

3.1. The prediction models

Based on the experimental results and a statistical analysis of variance, two models were determined for the maximum channel depth and thinning percentage of the bipolar plates, presented respectively in Equations (1) and (2). Regression calculations were performed using Design-Expert software package in order to fit the polynomial models to the output magnitude (i.e., responses). The highest order model with small P-values that is significant (i.e., P-values less than 0.05) and not aliased as well as a reasonable agreement between adjusted R-squared and predicted R-squared (within 0.2 of each other) were selected as a fitting model. However, the terms with a high p-value were neglected in order to reduce the unnecessary complexity of the present equations (the DOE approach and statistical analysis of the results are reported in more details in [34, 35]). As can be seen, the channel depth equation is of the second order and the thinning model is linear.

$$\text{Depth of channel (mm)} = 1.96 - 9.96 \times 10^{-3} \times - 0.04 \times P + 3.37 \times 10^{-3} \times D + 1.75 \times 10^{-4} \times T\ P + 1.25 \times 10^{-5} \times T^2 \quad (1)$$

$$\text{Thinning (\%)} = -29.20 + 0.12 \times T + 0.28 \times P\ 0.13 \times D \quad (2)$$

Where, T, P and D are temperature [˚C], gas pressure [bar] and process time [s], respectively. Table 4 lists the analysis of the variance output of both presented models. As shown, both models are accurate and significant, hence they could be used to navigate the design space.

3.2. The effects of process parameters on depth of channel

The effect of all three parameters (i.e. temperature, pressure and time) on the depth of the channel is shown in Figs. 5-7. By increasing each of the three parameters, the depth of the channel is increased. Temperature shows the most significant effect on the depth of the channel among other parameters. As the temperature rises, the aluminum sheet becomes more formable and experiences a plastic deformation with less gas pressure values. According to Fig. 5, the effect of the temperature on the channel depth is nonlinear. The slope of the curve has also begun to increase as the temperature increases. Referring to Fig. 6, the effect of gas pressure on the channel depth is linear. As the gas pressure increases, the induced stress of the sheet in the region that does not contact with the die increases, and as a result, the sheet tends to be drawn into the die cavity. However, it also causes an increase in the friction forces between the sheet and the die surfaces, which hinders the material flow into the channel. So, when the gas pressure increases in the factor of 100% the channel depth enhances by the factor of almost 50%. Additionally, by carefully considering Fig. 7, it can be seen that the process time of applying gas pressure, has a non-significant impact on the response. In fact, when the process time increases, the rate of the pressure increases and as a result, the strain rate of the plastic deformation reduces; and there is no sensitivity to the strain rate at these rates. The interactive effects of the gas temperature and pressure on the channel depth are illustrated in Fig. 8. Both factors have a positive influence on the channel depth. However, temperature has a more significant effect.

Table 4. Analysis of the variance output of two presented models

Parameter	Std. Dev.	R-squared	Adjusted R-squared	Predicted R-squared	Adeq. Precision
Depth of channel	0.03	0.964	0.952	0.851	31.92
Thinning (%)	0.83	0.982	0.979	0.969	64.58

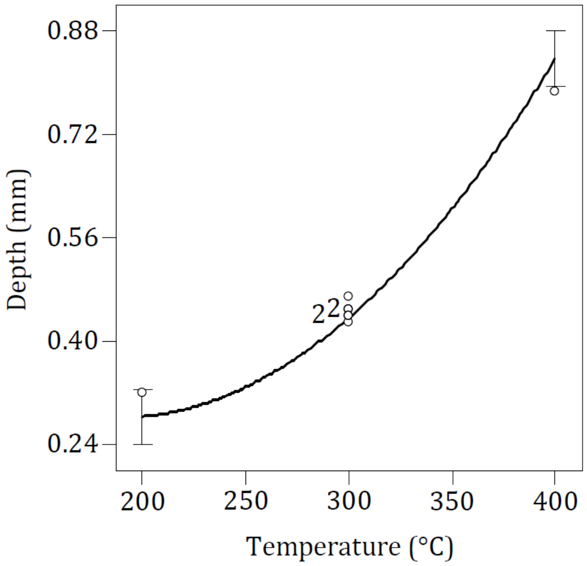

Fig. 5. Effect of gas temperature on the channel depth.

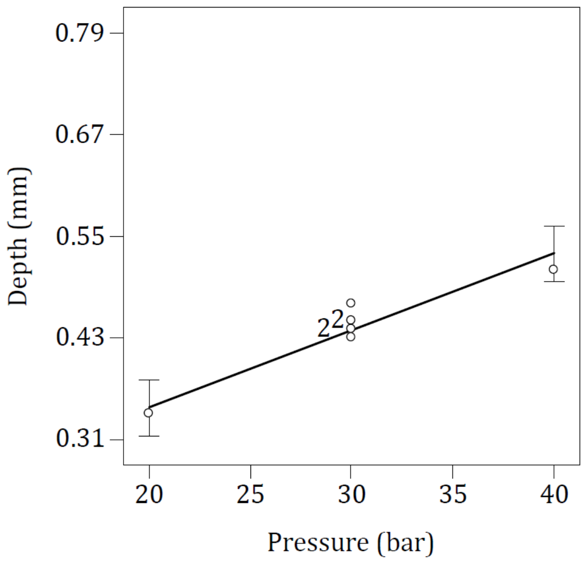

Fig. 6. Effect of gas pressure on the channel depth.

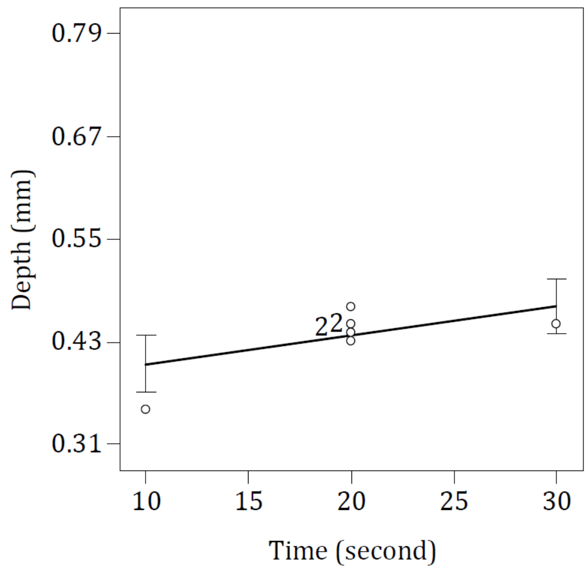

Fig. 7. Effect of process time on the channel depth.

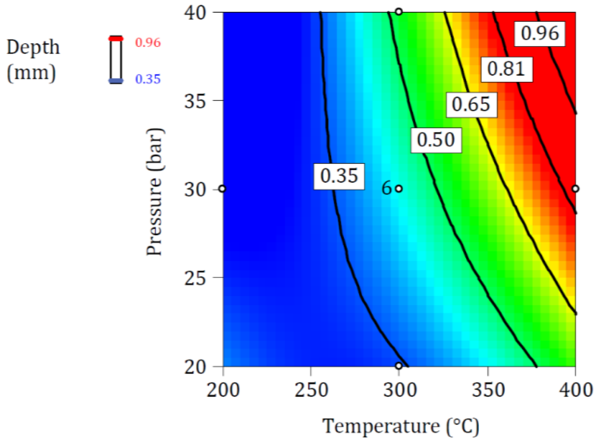

Fig. 8. The interactive effect of gas temperature and pressure on the channel depth.

3.3. The effects of process parameters on thinning

It is worth mentioning that high thinning percentages are not desirable and reduce the strength of the formed bipolar plates. The effect of process variables on thinning is shown in Fig. 9 and Figs. 11-12. The graphs show a similar effect, compared to the channel depth behavior. It was observed that as the temperature increases, the depth of the channel increases; thus, the sheet thickness decreases at the corner of the channel due to the constant volume of the material. In accordance with Fig. 9 temperature has a linear effect on the thinning percentage at the corner of the channel. To further investigate the effect of temperature on thinning, the thickness distribution of the central channel (i.e. the center of the Archimedean spiral) was measured for three specimens formed in 300, 350 and 400 degrees, as shown in Fig. 10. The minimum thickness at all temperatures is observed in the corner of the channel. As the temperature increases the center of the channel, that is not in contact with the die, experiences less thinning compared to the channel corners. This is attributed to the temperature differences between different sheet points, when the gas pressure is applied. In fact, the temperature gradient causes a change in the properties of the sheet material. The middle of the channel, which does not have contact with the die, the temperature is lower than the corners and hence, it is more resistant to deformation and thinning. For this reason, the deformation is concentrated in the corners of the channel and, by pulling this area through the applied gas pressure, the channel depth increases as does the thinning. The above-mentioned temperature gradient is more common at higher temperatures and, as a result, the difference in thinning between the corners and the central points of the channel is higher at higher temperatures. As the gas pressure increases, the thinning percentage increases, as well (Fig. 11). In fact, an increase in the final depth of the channel is supplied by the material flow in the channel corners. On the other hand, the changes in the process time have no significant effect on the thinning percentage of the product, due to the low sensitivity of the material to the strain rate. According to Fig. 12, the increase of the process time, which means the increase of the applied time of the gas pressure, increases the thinning with a slight slope.

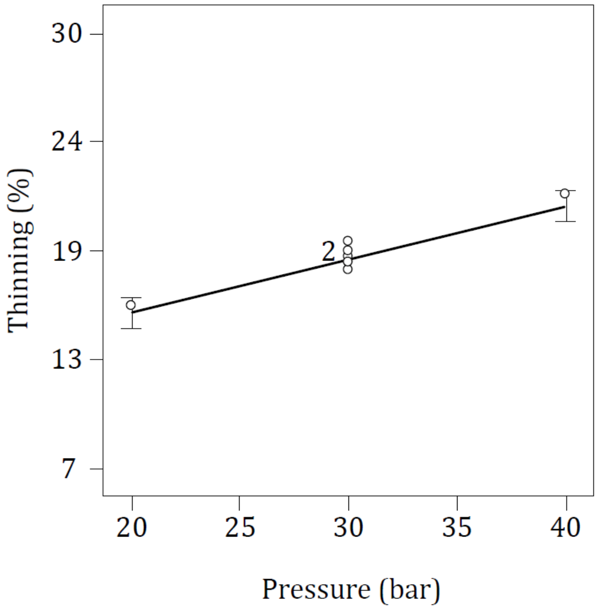

Fig. 11. Effect of gas pressure on the thinning

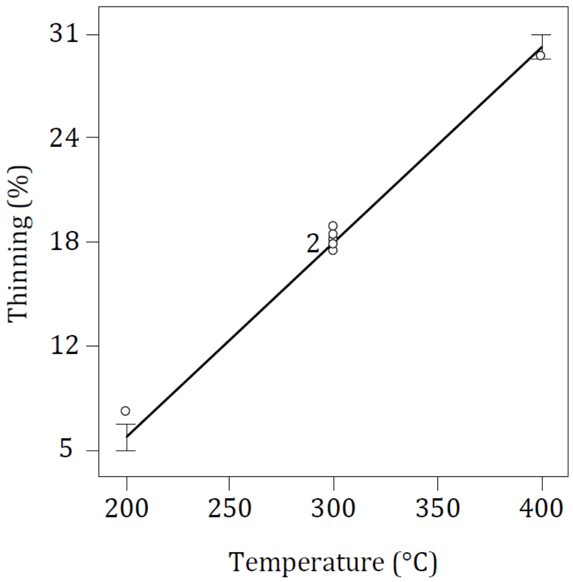

Fig. 9. Effect of gas temperature on the thinning.

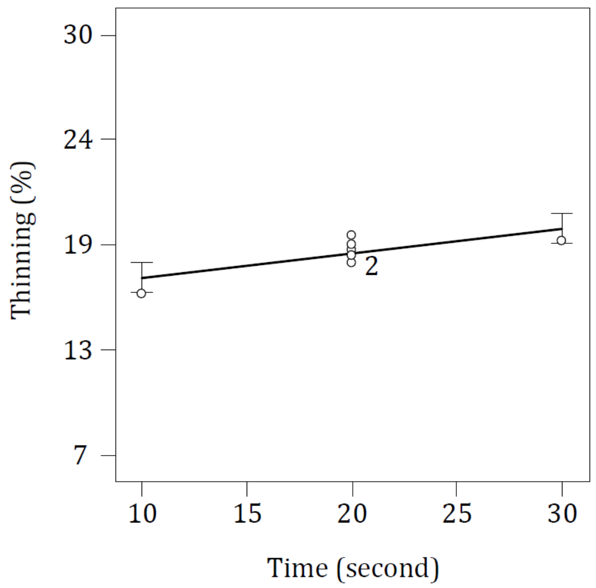

Fig. 12. Effect of process time on the thinning.

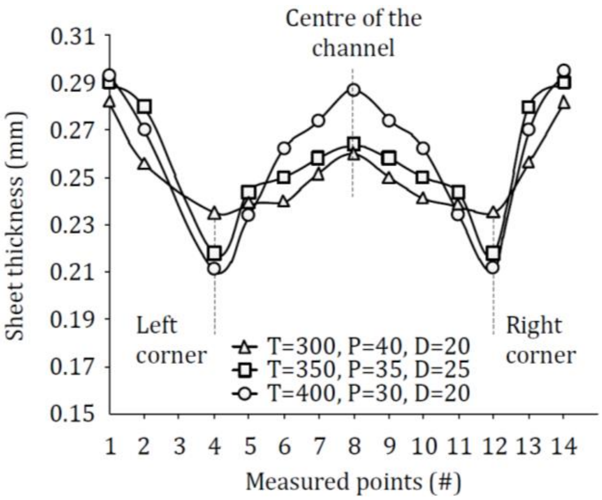

Fig. 10. Thickness distribution of the central channel.

3.4. Multi-objective optimization

In order to achieve the maximum depth of the channel in the bipolar plates, multi-objective optimization was performed. In this regard, a multiple response method called desirability is utilized using Design-Expert optimization package. In short, the above-mentioned method uses an objective function, called the desirability function, which reflects the desirable ranges for each response (the optimization approach is explained in more details in [36]). For the current study, the maximum allowed thinning of 20%

was considered. The optimum conditions for temperature, pressure and time were determined as 308˚C, 38 bar and 10 s, respectively. Taking into account these values, a 0.51 mm channel depth and 20% thinning is possible to be formed. In order to ensure the prediction of developed models, an experimental test was carried out with the mentioned process parameters. As a result, the depth of the channel of 0.48 mm and the thinning of 19.1% was achieved, which corresponds well with the prediction models.

4. Conclusions

In this study, the Archimedean spiral bipolar plates have been fabricated using a hot gas forming process:

1. The effects of input variables, including temperature, gas pressure, and process time, have been investigated on the final geometrical characteristics of the products.

2. It is observed that temperature has the most significant effect on the channel depth and thinning percentage. The higher the temperature, the more a specific depth of the channel can be achieved by applying less gas pressure values.

3. Additionally, the pressure applying time has almost no effect on the depth of the channel and its thinning.

4. Finally, an optimal amount of the parameters was determined to achieve the maximum depth of the channel. The optimal values are as follows: 308˚C, 38 bar and 10 s, which results in a channel with a depth of 0.48 mm and a thinning of 19.1%.

5. References

[1] H. N. Yu, J. W. Lim, J. Do Suh, A graphite-coated carbon fiber epoxy composite bipolar plate for polymer electrolyte membrane fuel cell, *Journal of Power Sources*, 196 (2011) 9868-9875.

[2] A. Hermann, T. Chaudhuri, P. Spagnol, Bipolar plates for PEM fuel cells: A review, *International Journal of Hydrogen Energy*, 30 (2005) 1297-1302.

[3] H. Tawfik, Y. Hung, D. Mahajan, Metal bipolar plates for PEM fuel cell: A review, *Journal of Power Sources*, 163 (2007) 755-767.

[4] B. G. Kim, J. W. Lim, A single-type aluminum/composite hybrid bipolar plate with surface modification for high efficiency PEMFC, *International Journal of Hydrogen Energy*, 36 (2011) 3087-3095.

[5] E. Wall, Multi-Year Research, Development and Demonstration Plan 2009-2015 with Program Activities to 2025, *Geothermal Technologies Office*, US (2012).

[6] S. Dhakate, S. Sharma, M. Borah, R. Mathur, T. Dhami, Expanded graphite-based electrically conductive composites as bipolar plate for PEM fuel cell, *International Journal of Hydrogen Energy*, 33 (2008) 7146-7152.

[7] S. P. Jung, C. I. Lee, C. C. Chen, W. S. Chang, C. C. Yang, Development of novel proton exchange membrane fuel cells using stamped metallic bipolar plates, *Journal of Power Sources*, 283 (2015) 429-442.

[8] V. V. Nikam, R. G. Reddy, Corrugated bipolar sheets as fuel distributors in PEMFC, *International Journal of Hydrogen Energy*, 31 (2006) 1863-1873.

[9] C. K. Jin, J. Y. Koo, C. G. Kang, Fabrication of stainless steel bipolar plates for fuel cells using dynamic loads for the stamping process and performance evaluation of a single cell, *International Journal of Hydrogen Energy*, 39 (2014) 21461-21469.

[10] Q. Hu, D. Zhang, H. Fu, K. Huang, Investigation of stamping process of metallic bipolar plates in PEM fuel cell-Numerical simulation and experiments, *International Journal of Hydrogen Energy*, 39 (2014) 13770-13776.

[11] M. P. Brady, M. A. Elhamid, G. Dadheech, J. Bradley, T. J. Toops, H. M. Meyer, P. F. Tortorelli, Manufacturing and performance assessment of stamped, laser welded, and nitrided FeCrV stainless steel bipolar plates for proton exchange membrane fuel cells, *International Journal of Hydrogen Energy*, 38 (2013) 4734-4739.

[12] M. G. Jung, Y. P. Jeon, C. G. Kang, Metallic Bipolar Plate Fabrication Process of Fuel Cell by Rubber Pad Forming and its Performance Evaluation, *Key Engineering Materials*, 535-536 (2013) 310-313.

[13] C. Jin, M. Jeong, C. Kang, Effect of process parameters on forming depth of channels in fuel cell bipolar plates fabricated using rubber forming process, *Materials Research Innovations*, 18 (2014) 462-472.

[14] L. Peng, P. Hu, X. Lai, D. Mei, J. Ni, Investigation of micro/meso sheet soft punch stamping process-simulation and experiments, *Materials & Design*, 30 (2009) 783-790.

[15] M. H. Dirikolu, E. Akdemir, Computer aided modelling of flexible forming process, *Journal of Materials Processing Technology*, 148 (2004) 376-381.

[16] Y. Liu, L. Hua, J. Lan, X. Wei, Studies of the deformation styles of the rubber-pad forming process used for manufacturing metallic bipolar plates, *Journal of Power Sources*, 195 (2010) 8177-8184.

[17] R. Kolahdooz, S. Asghari, S. Rashid-Nadimi, A. Amirfazli, Integration of finite element analysis and design of experiment for the investigation of critical factors in rubber pad forming of metallic bipolar plates for PEM fuel cells,

International Journal of Hydrogen Energy, 42 (2017) 575-589.

[18] M. Koç, S. Mahabunphachai, Feasibility investigations on a novel micro-manufacturing process for fabrication of fuel cell bipolar plates: Internal pressure-assisted embossing of micro-channels with in-die mechanical bonding, *Journal of Power Sources*, 172 (2007) 725-733.

[19] L. Peng, X. Lai, P. Hu, J. Ni, Flow channel shape optimum design for hydroformed metal bipolar plate in PEM fuel cell, *Journal of Power Sources*, 178 (2008) 223-230.

[20] F. Dundar, E. Dur, S. Mahabunphachai, M. Koc, Corrosion resistance characteristics of stamped and hydroformed proton exchange membrane fuel cell metallic bipolar plates, *Journal of Power Sources*, 195 (2010) 3546-3552.

[21] J. C. Hung, C. C. Lin, Fabrication of micro-flow channels for metallic bipolar plates by a high-pressure hydroforming apparatus, *Journal of Power Sources*, 206 (2012) 179-184.

[22] G. Palumbo, A. Piccininni, Numerical-experimental investigations on the manufacturing of an aluminium bipolar plate for proton exchange membrane fuel cells by warm hydroforming, *The International Journal of Advanced Manufacturing Technology*, 69 (2013) 731-742.

[23] D. Li, A. K. Ghosh, Biaxial warm forming behavior of aluminum sheet alloys, *Journal of Materials Processing Technology*, 145 (2004) 281-293.

[24] X. Fan, Z. He, P. Lin, S. Yuan, Microstructure, texture and hardness of Al-Cu-Li alloy sheet during hot gas forming with integrated heat treatment, *Materials & Design*, 94 (2016) 449-456.

[25] M. Keigler, H. Bauer, D. Harrison, A. K. De Silva, Enhancing the formability of aluminium components via temperature controlled hydroforming, *Journal of Materials Processing Technology*, 167 (2005) 363-370.

[26] Z. B. He, B. G. Teng, C. Y. Che, Z. B. Wang, K. L. Zheng, S. J. Yuan, Mechanical properties and formability of TA2 extruded tube for hot metal gas forming at elevated temperature, *Transactions of Nonferrous Metals Society of China*, 22 (2012) 479-484.

[27] Z. B. He, X. B. Fan, S. Fei, K. L. Zheng, Z. B. Wang, S. J. Yuan, Formability and microstructure of AA6061 Al alloy tube for hot metal gas forming at elevated temperature, *Transactions of Nonferrous Metals Society of China*, 22 (2012) 364-369.

[28] L. Gang, W. D. Zhang, Z. B. He, S. J. Yuan, L. Zhe, Warm hydroforming of magnesium alloy tube with large expansion ratio within non-uniform temperature field, *Transactions of Nonferrous Metals Society of China*, 22 (2012) 408-415.

[29] T. Maeno, K. I. Mori, K. Fujimoto, Hot gas bulging of sealed aluminium alloy tube using resistance heating, *Manufacturing Review*, 1 (2014) 210-218.

[30] M. Vahdati, M. Moradi, M. Shamsborhan, Modeling and optimization of the yield strength and tensile strength of Al7075 butt joint produced by FSW and SFSW using RSM and desirability function method, *Transactions of the Indian Institute of Metals*, 73 (2020) 2587-2600.

[31] A. H. Roohi, S. J. Hashemi, M. Allahyari, Hot metal gas forming of closed-cell aluminum foam sandwich panels, *Transactions of the Indian Institute of Metals*, 73 (2020) 2231-2238.

[32] M. Vahdati, M. Moradi, Statistical analysis and optimization of the yield strength and hardness of surface composite Al7075/Al2O3 produced by FSP via RSM and desirability approach, *Iranian Journal of Materials Forming*, 7 (2020) 32-45.

[33] A. Mostafapour, M. Moradi, H. Kamali, M. Saleh Meiabadi, Multi-response optimization of the mechanical and metallurgical properties of Al7075-T6 deposition process on Al2024-T351 by friction surfacing using RSM and the desirability approach, *Iranian Journal of Materials Forming*, 7 (2020) 100-115.

[34] A. H. Roohi, H. Moslemi Naeini, M. Hoseinpour Gollo, M. Soltanpour, S. Bruschi, A. Ghiotti, Forming of closed-cell aluminum foams under thermal loadings: experimental investigation, *The International Journal of Advanced Manufacturing Technology*, 95 (2018) 3919-3928.

[35] A. H. Roohi, H. M. Naeini, M. H. Gollo, M. Soltanpour, M. Abbaszadeh, On the random-based closed-cell metal foam modeling and its behavior in laser forming process, *Optics & Laser Technology*, 72 (2015) 53-64.

[36] Software D-E Help Section.